

Notes

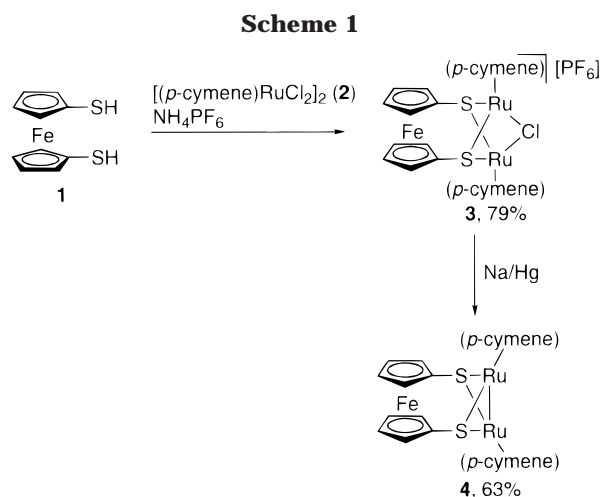
Synthesis and Structures of 1,1'-Ferrocenedithiolato-Bridged Di- and Trinuclear Ruthenium Complexes

Shin Takemoto, Shigeki Kuwata, Yoshiaki Nishibayashi,[†] and Masanobu Hidai*Department of Chemistry and Biotechnology, Graduate School of Engineering,
The University of Tokyo, Hongo, Bunkyo-ku, Tokyo 113-8656, Japan

Received April 3, 2000

Summary: The 1,1'-ferrocenedithiolato-bridged (arene)-ruthenium(I) complex $[\{(p\text{-cymene})\text{Ru}\}_2(\mu_2\text{-S}_2\text{fc})]$ (**4**; $p\text{-cymene}$ = 4-isopropyltoluene, S_2fc = 1,1'-ferrocenedithiolato) was synthesized by the reaction of 1,1'-ferrocenedithiol (**1**) with $[(p\text{-cymene})\text{RuCl}_2]_2$ (**2**) and subsequent reduction with sodium amalgam; reactions of **4** with HOTf and MeOTf (OTf = OSO_2CF_3) afforded the hydrido complex $[\{(p\text{-cymene})\text{Ru}\}_2(\mu_2\text{-H})(\mu_2\text{-S}_2\text{fc})][\text{OTf}]$ (**5**) and the thiolato–thioether complex $[\{(p\text{-cymene})\text{Ru}\}_2(\mu_2\text{-SfcSMe})][\text{OTf}]$ (**6**), respectively. On the other hand, treatment of $[\text{Cp}^*\text{RuCl}]_4$ (**7**; Cp^* = $\eta^5\text{-C}_5\text{Me}_5$) with 1,2,3-trithia[3]ferrocenophane (**8**) resulted in the formation of the (1,1'-ferrocenedithiolato)(sulfido)triruthenium cluster $[(\text{Cp}^*\text{Ru})_3(\mu_3\text{-S})(\mu_3\text{-S}_2\text{fc})(\mu_2\text{-Cl})][\text{FeCl}_4]$ (**9**).

In our continuing studies on sulfur-bridged polynuclear complexes,¹ we have synthesized a series of thiolato-bridged diruthenium, dirhodium, and diiridium complexes² and revealed their catalytic ability for transformations of various substrates such as alkynes and allylic compounds.³ Owing to the presence of the strongly bridging thiolato ligands, the dinuclear structures of these complexes are preserved throughout the catalytic reactions. As an extension of these studies, we have recently prepared ferrocenedithiolato-bridged diruthenium complexes⁴ and 1,1'-ferrocenedithiolato-bridged M_2 and RuM complexes (M = Ni, Pd, Pt),⁵ since the complexes having cylindrical and redox-active ferrocene



moieties such as ferrocenylphosphine complexes are known to show unique reactivities.⁶ Here we describe the synthesis and reactivities of di- and triruthenium complexes with a 1,1'-ferrocenedithiolato ligand.

Reaction of the (arene)diruthenium complex $[(p\text{-cymene})\text{RuCl}_2]_2$ (**2**) with 1 equiv of 1,1'-ferrocenedithiol (**1**) and subsequent anion metathesis with NH_4PF_6 led to the formation of the diruthenium complex $[\{(p\text{-cymene})\text{Ru}\}_2(\mu_2\text{-Cl})(\mu_2\text{-S}_2\text{fc})][\text{PF}_6]$ (**3**) in 79% yield (Scheme 1). The ^1H NMR spectrum of **3** confirms the presence of the ferrocenedithiolato and $p\text{-cymene}$ ligands in a ratio of 1:2, and the simple spectral feature is consistent with the diruthenium structure of **3** shown in Scheme 1. The closely related bis(benzenedithiolato) complex $[\{(\text{C}_6\text{Me}_6)\text{Ru}\}_2(\mu_2\text{-Cl})(\mu_2\text{-SPh})_2]\text{Cl}$,⁷ as well as the tris(thiolato) complexes $[\{(\text{arene})\text{Ru}\}_2(\mu_2\text{-SR})_3]^+$ (arene = C_6Me_6 , $p\text{-cymene}$, C_6H_6 ; R = Ph, Et)^{7,8} has

* To whom correspondence should be addressed at the Department of Materials Science and Technology, Faculty of Industrial Science and Technology, Science University of Tokyo, Noda, Chiba 278-8510, Japan.

[†] Present address: Department of Energy and Hydrocarbon Chemistry, Graduate School of Engineering, Kyoto University, Sakyo-ku, Kyoto 606-8501, Japan.

(1) Hidai, M.; Kuwata, S.; Mizobe, Y. *Acc. Chem. Res.* **2000**, *33*, 46.
(2) (a) Hidai, M.; Mizobe, Y.; Matsuzaka, H. *J. Organomet. Chem.* **1994**, *473*, 1. (b) Hidai, M.; Mizobe, Y. In *Transition Metal Sulfur Chemistry*; Stiefel, E. I., Matsumoto, K., Eds.; American Chemical Society: Washington, DC, 1996; p 310. (c) Nishio, M.; Matsuzaka, H.; Mizobe, Y.; Hidai, M. *Inorg. Chim. Acta* **1997**, *263*, 119. (d) Nishio, M.; Mizobe, Y.; Matsuzaka, H.; Hidai, M. *Inorg. Chim. Acta* **1997**, *265*, 59. (e) Iwasa, T.; Shimada, H.; Takami, A.; Matsuzaka, H.; Ishii, Y.; Hidai, M. *Inorg. Chem.* **1999**, *38*, 2851. (f) Matsukawa, S.; Kuwata, S.; Hidai, M. *Inorg. Chem.* **2000**, *39*, 791.

(3) (a) Nishibayashi, Y.; Yamanashi, M.; Takagi, Y.; Hidai, M. *Chem. Commun.* **1997**, 859. (b) Qü, J.-P.; Masui, D.; Ishii, Y.; Hidai, M. *Chem. Lett.* **1998**, 1003.

(4) Matsuzaka, H.; Qü, J.-P.; Ogino, T.; Nishio, M.; Nishibayashi, Y.; Ishii, Y.; Uemura, S.; Hidai, M. *J. Chem. Soc., Dalton Trans.* **1996**, 4307.

(5) Takemoto, S.; Kuwata, S.; Nishibayashi, Y.; Hidai, M. *Inorg. Chem.* **1998**, *37*, 6428.

(6) (a) Hayashi, T. In *Ferrocenes*; Togni, A., Hayashi, T., Eds.; VCH: Weinheim, Germany, 1995; Chapter 2, and references therein. (b) Nishibayashi, Y.; Segawa, K.; Ohe, K.; Uemura, S. *Organometallics* **1996**, *15*, 370. (c) Hembre, R. T.; McQueen, J. S.; Day, V. W. *J. Am. Chem. Soc.* **1996**, *118*, 798. (d) Nishibayashi, Y.; Takei, I.; Uemura, S.; Hidai, M. *Organometallics* **1999**, *18*, 2291. (e) Nishibayashi, Y.; Takei, I.; Hidai, M. *Organometallics* **1997**, *16*, 3091.

(7) Schacht, H. T.; Hältiwanger, R. C.; Rakowski DuBois, M. *Inorg. Chem.* **1992**, *31*, 1728.

(8) (a) Gould, R. O.; Stephenson, T. A.; Tocher, D. A. *J. Organomet. Chem.* **1984**, *263*, 375. (b) Mashima, K.; Mikami, A.; Nakamura, A. *Chem. Lett.* **1992**, 1795.

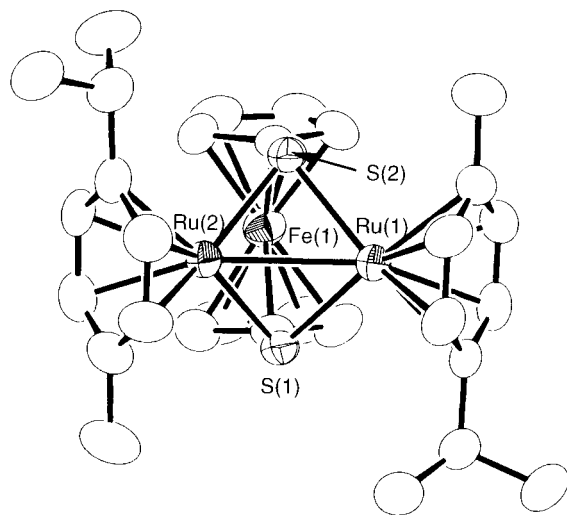


Figure 1. ORTEP drawing of the cationic part of **5**. Hydrogen atoms are omitted for clarity.

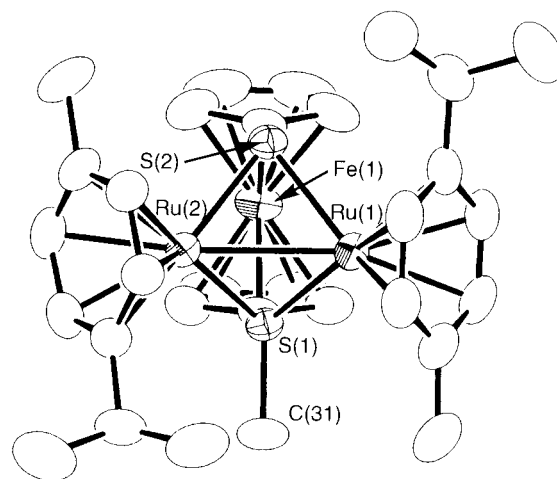
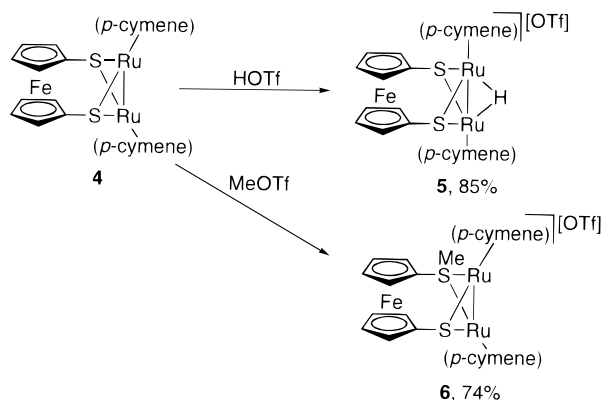


Figure 2. ORTEP drawing of the cationic part of **6**. Hydrogen atoms are omitted for clarity.

Scheme 2



already been reported. The cyclic voltammogram of **3** exhibits a reversible oxidation wave at 0.71 V (vs saturated calomel electrode (SCE)) and an irreversible reduction wave at -1.20 V. The former can be assigned to the Fe(II/III) redox couple. Attempts to isolate the oxidized product 3^+ by using oxidants such as AgPF_6 and NOBF_4 , however, have failed.

On the other hand, reduction of **3** with an excess of Na/Hg in THF at room temperature resulted in the isolation of the Ru(I)/Ru(I) complex $[\{(\text{p-cymene})\text{Ru}\}_2(\mu_2\text{-S}_2\text{fc})]$ (**4**) in 63% yield (Scheme 1). The feature of the ^1H NMR spectrum of **4** resembles that of the parent complex **3**, suggesting that the symmetrical diruthenium structure of **3** is preserved in **4**. The diamagnetic nature of **4** indicates the presence of a Ru(I)–Ru(I) single bond. Complex **4** is a thiolato-bridged diruthenium(I) complex with arene ligands, whereas thiolato-bridged diruthenium(I) centers are well-known to bind CO ,⁹ as exemplified by $[\{\text{Ru}(\text{CO})_3\}_2(\mu_2\text{-S}_2\text{fc})]$.^{9a}

When **4** is treated with HOTf, protonation to the Ru(I)–Ru(I) bond takes place to afford the hydrido-

Table 1. Selected Bond Lengths (Å) and Angles (deg) for **5** and **6**

	5	6
Ru(1)–Ru(2)	2.7698(7)	2.7489(5)
Ru(1)–S(1)	2.350(2)	2.271(1)
Ru(1)–S(2)	2.358(2)	2.342(1)
Ru(2)–S(1)	2.359(2)	2.271(1)
Ru(2)–S(2)	2.363(2)	2.335(1)
S(1)–C(31)		1.801(5)
Ru(2)–Ru(1)–S(1)	54.12(4)	52.76(3)
Ru(2)–Ru(1)–S(2)	54.16(4)	53.88(3)
S(1)–Ru(1)–S(2)	85.42(5)	82.56(4)
Ru(1)–Ru(2)–S(1)	53.83(4)	52.75(3)
Ru(1)–Ru(2)–S(2)	53.99(4)	54.12(3)
S(1)–Ru(2)–S(2)	85.11(5)	82.71(4)
Ru(1)–S(1)–Ru(2)	72.06(5)	74.49(4)
Ru(1)–S(2)–Ru(2)	71.85(5)	72.00(4)
Ru(1)–S(1)–C(31)		119.9(2)
Ru(2)–S(1)–C(31)		119.9(2)

Table 2. Selected Interatomic Distances (Å) and Angles (deg) for **9**

Ru(1)–Ru(2)	2.8264(8)	Ru(1)–S(1)	2.280(2)
Ru(1)–S(2)	2.285(2)	Ru(1)–Cl(1)	2.461(2)
Ru(2)–S(1)	2.349(2)	Ru(2)–S(2)	2.319(2)
Ru(1)···Ru(1*)	3.496(1)		
S(1)–Ru(1)–S(2)	106.13(7)	S(1)–Ru(1)–Cl(1)	93.65(7)
Cl(1)–Ru(1)–S(2)	81.70(6)	S(1)–Ru(2)–S(1*)	99.20(8)
S(1)–Ru(2)–S(2)	102.86(6)	Ru(1)–Cl(1)–Ru(1*)	90.49(8)
Ru(1)–S(2)–Ru(1*)	99.82(9)	Ru(1)–S(1)–Ru(2)	75.25(5)
Ru(1)–S(2)–Ru(2)	75.75(6)	Ru(1)–Ru(2)–Ru(1*)	76.40(3)

bridged diruthenium(II) complex $[\{(\text{p-cymene})\text{Ru}\}_2(\mu_2\text{-H})(\mu_2\text{-S}_2\text{fc})][\text{OTf}]$ (**5**; Scheme 2). The ^1H NMR spectrum of **5** shows a hydrido resonance at -11.77 ppm. Resonances for the two *p*-cymene ligands appear equivalent even at -50 °C, suggesting the bridging nature of the hydrido ligand. The dinuclear structure of **5** has further been confirmed by an X-ray diffraction analysis (Figure 1 and Table 1), although the hydrido hydrogen atom could not be located. The Ru(1)–Ru(2) distance of 2.7698(7) Å is consistent with the presence of a Ru–H–Ru three-center–two-electron bond, whereas the long Fe–Ru distances of 4.316(1) and 4.283(1) Å indicate the absence of any direct bonding interaction between these atoms. On the other hand, the reaction of **4** with MeOTf results in S-alkylation, giving the thiolato-thioether complex $[\{(\text{p-cymene})\text{Ru}\}_2(\mu_2\text{-SfcSMe})][\text{OTf}]$ (**6**) as shown in Scheme 2. The SMe resonance appears

(9) See, for example: (a) Cullen, W. R.; Talaba, A.; Rettig, S. J. *Organometallics* **1992**, *11*, 3152. (b) Cabeza, J. A.; Martínez-García, M. A.; Riera, V.; Ardura, D.; García-Granda, S. *Organometallics* **1998**, *17*, 1471. (c) Shiu, K.-B.; Wang, S.-L.; Liao, F.-L.; Chiang, M. Y.; Peng, S.-M.; Lee, G.-H.; Wang, J.-C.; Liou, L.-S. *Organometallics* **1998**, *17*, 1790. (d) Cabeza, J. A.; Martínez-García, M. A.; Riera, V.; Ardura, D.; García-Granda, S.; Van der Maelen, J. F. *Eur. J. Inorg. Chem.* **1999**, 1133. (e) Seyferth, D.; Hames, B. *Inorg. Chim. Acta* **1983**, *77*, L1.

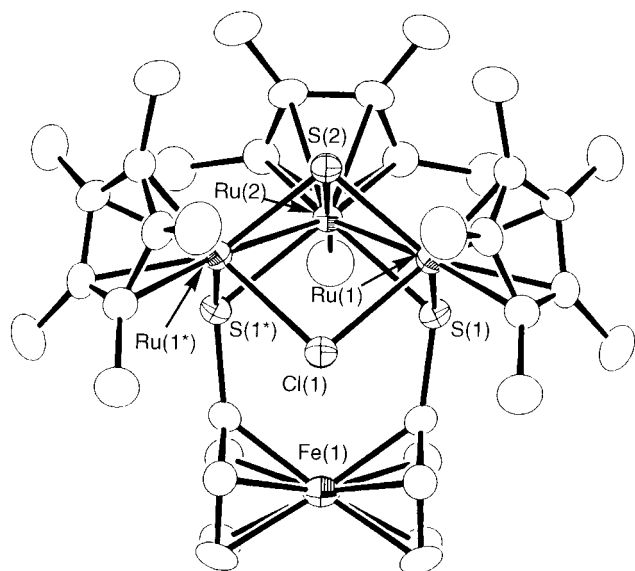
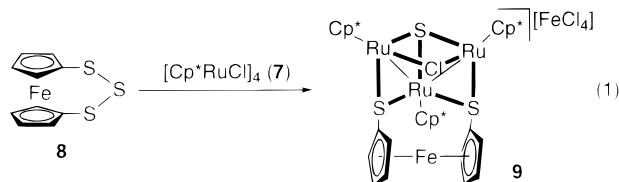


Figure 3. ORTEP drawing of the cationic part of **9**. Hydrogen atoms are omitted for clarity.

at 2.92 ppm in the ^1H NMR spectrum of **6**, and the C_s symmetry of **6** is deduced by the spectrum. To determine the detailed structure of **6**, an X-ray analysis has been carried out (Figure 2). The Ru(1)–Ru(2) distance of 2.7489(5) Å is comparable to that in $[\{\text{Ru}(\text{CO})_3\}_2(\mu_2\text{-S}_2\text{fc})]$ (2.6812(7) Å),^{9a} suggesting the presence of a Ru(I)–Ru(I) bond. The Ru–S_{thioether} distances (2.271 Å (mean)) are slightly shorter than the Ru–S_{thiolato} distances (2.339 Å (mean)). The reactivities of the thiolato-bridged (arene)ruthenium complex **4** described above parallel those of the carbonyl complex $[\{\text{Ru}(\text{CO})_3\}_2(\mu_2\text{-S}_2\text{C}_6\text{H}_4)]^{9b}$ and the isoelectronic iridium(II) complex $[(\text{Cp}^*\text{Ir})_2(\mu\text{-SPR}^i)_2]^{2c,d}$.

Reaction of **1** with $[\text{Cp}^*\text{RuCl}]_4$ (**7**) did not give any characterizable product. However, 1,2,3-trithia[3]ferrocenophane (**8**) reacts with **7** in an Fe:Ru ratio of 1:1.7 to afford the 1,1'-ferrocenedithiolato- and sulfido-bridged triruthenium cluster $[(\text{Cp}^*\text{Ru})_3(\mu_3\text{-S})(\mu_3\text{-S}_2\text{fc})(\mu_2\text{-Cl})][\text{FeCl}_4]$ (**9**) in 25% yield based on the Ru atom (eq 1).



The molecular structure of **9** has been determined by X-ray crystallography (Figure 3 and Table 2). As expected for the 50e clusters, **9** has an open triangular Ru₃ core with only two Ru–Ru bonds (Ru(1)–Ru(2) and Ru(1*)–Ru(2)). The Ru^{III}Ru^{IV} triangle is capped by a sulfido ligand, and the three Ru atoms are bridged by two thiolato sulfur atoms and a chloro ligand to form an incomplete cubane-type core. Related core structures are observed in $[(\text{Cp}^*\text{Rh})_3(\mu_3\text{-S})(\mu_2\text{-Cl})_2(\mu_2\text{-SPR}^i)][\text{OTf}]^{2e}$ and $[(\text{tmtRu})_3(\mu_3\text{-S})(\mu_2\text{-Cl})_3][\text{PF}_6]$ (tmt = tetramethylthiophene),¹⁰ although there seem to be no direct metal–metal interactions in these complexes. Obviously, the

iron atom in the FeCl_4^{2-} anion is derived from the ferrocenophane **8**; however, the mechanism for formation of this anion as well as the fate of the cyclopentadienyl groups around the iron atom is unclear at present.

In summary, we have synthesized a series of 1,1'-ferrocenedithiolato-bridged di- and triruthenium complexes. Their unique structures are, at least partly, due to the presence of the chelating ferrocenedithiolato ligand.

Experimental Section

General Considerations. All manipulations were performed under an atmosphere of nitrogen using standard Schlenk-tube techniques unless otherwise specified. Solvents were dried and distilled before use. The compounds **1**,¹¹ **2**,¹² **7**,¹³ and **8**¹¹ were prepared according to the literature.

^1H NMR spectra were recorded on a JEOL JNM-EX-270 or JNM-LA400 spectrometer. Elemental analyses were performed on a Perkin-Elmer 2400 Series II CHN analyzer. Amounts of the solvent molecules were determined not only by elemental analyses but also by ^1H NMR spectroscopy. Electrochemical measurements were made with Hokuto Denko instrumentation (HA-501 potentiostat and HB-105 function generator) using a glassy-carbon working electrode; potentials were measured in CH_2Cl_2 –0.1 M Bu_4NBF_4 vs SCE as reference.

Preparation of $[(p\text{-cymene})\text{Ru}]_2(\mu_2\text{-Cl})(\mu_2\text{-S}_2\text{fc})[\text{PF}_6]\cdot\text{CH}_2\text{Cl}_2$ (3**· CH_2Cl_2).** To a solution of **2** (850 mg, 1.39 mmol) in CH_2Cl_2 –MeOH (30 mL/10 mL) were added **1** (350 mg, 1.39 mmol) and NH_4PF_6 (326 mg, 2.00 mmol), and the mixture was stirred for 4 h at room temperature. After removal of the solvents in vacuo, the residue was extracted with CH_2Cl_2 (40 mL). Slow diffusion of hexanes into the concentrated extract gave **3**· CH_2Cl_2 as a red microcrystalline solid (1.08 g, 79%). ^1H NMR (acetone- d_6): δ 6.11, 5.76 (d, 4H each, J = 5.6 Hz, $\text{MeC}_6\text{H}_4\text{Pr}^i$), 4.69, 4.11 (t, 4H each, J = 2.0 Hz, C_5H_4), 3.03 (sept, 2H, J = 6.9 Hz, CHMe_2), 2.51 (s, 6H, $\text{MeC}_6\text{H}_4\text{Pr}^i$), 1.37 (d, 12H, J = 6.9 Hz, CHMe_2). Anal. Calcd for $\text{C}_{31}\text{H}_{38}\text{Cl}_3\text{F}_6\text{PS}_2\text{FeRu}_2$: C, 37.84; H, 3.89. Found: C, 37.72; H, 4.07.

Preparation of $[(p\text{-cymene})\text{Ru}]_2(\mu_2\text{-S}_2\text{fc})$ (4**).** In a 20 mL Schlenk flask containing Na/Hg (2.1%, 3.8 g, 3.4 mmol) and THF (8 mL), **3**· CH_2Cl_2 (296 mg, 0.301 mmol) was added at room temperature and the mixture was stirred for 1 h. After addition of hexanes (2 mL), the reddish brown solution was filtered. The filtrate was evaporated to dryness and extracted with benzene (5 mL). MeOH was layered on the concentrated extract, and the mixture was cooled to -23°C , giving **4** as red-brown crystals (130.6 mg, 63%). ^1H NMR (C_6D_6): δ 5.47, 5.36 (d, 4H each, J = 5.6 Hz, $\text{MeC}_6\text{H}_4\text{Pr}^i$), 4.68, 3.92 (t, 4H each, J = 1.8 Hz, C_5H_4), 2.45 (sept, 2H, J = 6.9 Hz, CHMe_2), 1.96 (s, 6H, $\text{MeC}_6\text{H}_4\text{Pr}^i$), 1.22 (d, 12H, J = 6.9 Hz, CHMe_2). Anal. Calcd for $\text{C}_{30}\text{H}_{36}\text{S}_2\text{FeRu}_2$: C, 50.13; H, 5.05. Found: C, 50.31; H, 5.10.

Preparation of $[(p\text{-cymene})\text{Ru}]_2(\mu_2\text{-H})(\mu_2\text{-S}_2\text{fc})[\text{OTf}]$ (5**).** To a solution of **4** (71.8 mg, 0.100 mmol) in toluene (3 mL) was added HOTf (16.5 mg, 0.110 mmol) at -65°C . The mixture was slowly warmed to room temperature and stirred further for 2 h at this temperature. The solvent was removed in vacuo, and the residue was recrystallized from CH_2Cl_2 –hexanes to afford dark red crystals of **5** (73.9 mg, 85%). ^1H NMR (acetone- d_6): δ 6.54, 6.36 (d, 4H each, J = 6.0 Hz, $\text{MeC}_6\text{H}_4\text{Pr}^i$), 4.82, 4.01 (t, 4H each, J = 1.8 Hz, C_5H_4), 2.56 (sept, 2H, J = 6.4 Hz, CHMe_2), 2.23 (s, 6H, $\text{MeC}_6\text{H}_4\text{Pr}^i$), 1.20

(10) Lockemeyer, J. R.; Rauchfuss, T. B.; Rheingold, A. L.; Wilson, S. R. *J. Am. Chem. Soc.* **1989**, *111*, 8828.

(11) Bishop, J. J.; Davison, A.; Katcher, M. L.; Lichtenberg, D. W.; Merrill, R. E.; Smart, J. C. *J. Organomet. Chem.* **1971**, *27*, 241.

(12) Bennett, M. A.; Huang, T.-N.; Matheson, T. W.; Smith, A. K. *Inorg. Synth.* **1982**, *21*, 74.

(13) Fagan, P. J.; Ward, M. D.; Calabrese, J. C. *J. Am. Chem. Soc.* **1989**, *111*, 1698.

(d, 12H, $J = 6.4$ Hz, CHMe_2), -11.77 (s, RuH). Anal. Calcd for $\text{C}_{31}\text{H}_{37}\text{S}_3\text{O}_3\text{F}_3\text{FeRu}_2$: C, 42.86; H, 4.29. Found: C, 42.72; H, 4.23.

Preparation of $[(p\text{-cymene})\text{Ru}]_2(\mu_2\text{-SfcSMe})[\text{OTf}]$ (6**).** To a solution of **4** (71.8 mg, 0.100 mmol) in toluene (3 mL) was added MeOTf (18.1 mg, 0.110 mmol) at -65°C , and the mixture was slowly warmed to room temperature and stirred further for 1 h at this temperature. The solvent was removed in vacuo, and the residue was recrystallized from CH_2Cl_2 –hexanes to afford dark red crystals of **6** (65.3 mg, 74%). ^1H NMR (CDCl_3): δ 6.01, 5.88, 5.83, 5.71 (d, 2H each, $J = 5.9$ Hz, $\text{MeC}_6\text{H}_4\text{Pr}^i$), 4.73, 4.39, 4.05, 3.96 (t, 2H each, $J = 1.7$ Hz, C_5H_4), 2.92 (s, 3H, SMe), 2.64 (sep, 2H, $J = 6.8$ Hz, CHMe_2), 2.27 (s, 6H, $\text{MeC}_6\text{H}_4\text{Pr}^i$), 1.31 (d, 12H, $J = 6.8$ Hz, CHMe_2). Anal. Calcd for $\text{C}_{32}\text{H}_{39}\text{S}_3\text{O}_3\text{F}_3\text{FeRu}_2$: C, 43.54; H, 4.45. Found: C, 43.45; H, 4.42.

Preparation of $[(\text{Cp}^*\text{Ru})_3(\mu_3\text{-S})(\mu_3\text{-S}_2\text{fc})(\mu_2\text{-Cl})][\text{FeCl}_4]$ (9**).** To a suspension of **7** (59.7 mg, 0.055 mmol) in THF (8 mL) was added **8** (36.9 mg, 0.13 mmol), and the mixture was stirred for 4 h at room temperature. The dark brown solid that formed was collected and washed with THF. Recrystallization from acetonitrile–diethyl ether gave **9** as dark brown crystals (22 mg, 0.018 mmol, 25% based on the Ru atom). ^1H NMR (CD_3CN): δ 5.68, 4.49, 4.34, 4.21 (m, 2H each, C_5H_4), 1.80 (s, 15H, C_5Me_5), 1.65 (s, 30H, C_5Me_5). Anal. Calcd for $\text{C}_{40}\text{H}_{53}\text{Cl}_5\text{S}_3\text{Fe}_2\text{Ru}_3$: C, 39.31; H, 4.37. Found: C, 39.05; H, 4.91.

X-ray Diffraction Studies. Crystals were sealed in glass capillaries under an argon atmosphere and used for data collection. Diffraction data were collected on a Rigaku AFC-7R four-circle automated diffractometer equipped with a graphite-monochromated Mo $K\alpha$ ($\lambda = 0.71069$ Å) source at room temperature using the ω – 2θ scan technique ($5^\circ < 2\theta < 50^\circ$ for **5**, $5^\circ < 2\theta < 55^\circ$ for **6** and **9**). Accurate cell dimensions of each crystal were determined by least-squares refinement of 21, 25, and 20 machine-centered reflections for **5**, **6**, and **9**, respectively. Empirical absorption corrections based on Ψ scans and Lorentz-polarization corrections were applied. The intensities of 3 check reflections were monitored every 150 reflections for each crystal, which showed no significant decay for **5** and **6** but a steady decrease in intensities for **9** during data corrections (average 4.6% decrease for 3 check reflections at the final stage). Thus, a decay correction was applied for **9**. Details of the X-ray diffraction study are summarized in Table 3.

The structure solution and refinement were performed by using the TEXSAN¹⁴ program package. The structures were solved by a combination of heavy-atom Patterson methods (PATY¹⁵) and subsequent Fourier techniques (DIRDIF94¹⁶). All non-hydrogen atoms were found from the difference Fourier

Table 3. Crystallographic Data for **5**, **6**, and **9**

	5	6	9
formula	$\text{C}_{31}\text{H}_{37}\text{F}_3\text{O}_3\text{S}_3\text{FeRu}_2$	$\text{C}_{32}\text{H}_{39}\text{F}_3\text{O}_3\text{S}_3\text{FeRu}_2$	$\text{C}_{40}\text{H}_{53}\text{Cl}_5\text{S}_3\text{Fe}_2\text{Ru}_3$
fw	868.79	882.82	1222.21
space group	$C2/c$	$C2/c$	$Pnma$
cryst syst	monoclinic	monoclinic	orthorhombic
cryst color	dark red	dark red	dark brown
cryst dimens, mm	$0.80 \times 0.50 \times 0.30$	$0.90 \times 0.70 \times 0.20$	$0.20 \times 0.20 \times 0.20$
a , Å	18.921(3)	31.593(5)	22.024(4)
b , Å	11.554(1)	11.387(4)	16.185(3)
c , Å	30.806(4)	19.206(6)	12.373(3)
β , deg	101.940(10)	97.56(2)	90
V , Å ³	6589(1)	6849(3)	4410(2)
Z	8	8	4
ρ_{calcd} , g cm ^{−3}	1.751	1.712	1.840
$F(000)$, e	3488	3552	2440
μ (Mo $K\alpha$)	15.78	15.19	21.20
no. of rflns measd	6318	8400	4031
no. of unique rflns	6115	8249	4031
transmissn	0.9080–	0.7472–	0.9005–
factors	0.9997	1.0000	0.9992
no. of rflns used ($I > 3\sigma(I)$)	4252	5604	2767
no. of variables	389	398	254
R^a	0.043	0.035	0.036
R_w^a	0.046	0.037	0.028
GOF	1.96	1.78	1.50
max residual density, e Å ^{−3}	1.96	1.40	0.87

$$^a R = \sum ||F_o| - |F_c|| / \sum |F_o|; R_w = [\sum w(|F_o| - |F_c|)^2 / \sum wF_o^2]^{1/2}.$$

maps and refined by full-matrix least-squares techniques with anisotropic thermal parameters. The hydrogen atom of the hydrido ligand in **5** was not located, while all other hydrogen atoms were placed at calculated positions and included in the final stage of refinements with fixed parameters.

Acknowledgment. We acknowledge financial support by a Grant-in-Aid for Specially Promoted Research (No. 09102004) from The Ministry of Education, Science, Sports, and Culture of Japan.

Supporting Information Available: Tables of atomic coordinates, anisotropic thermal parameters, and all bond lengths and angles for **5**, **6**, and **9**. This material is available free of charge via the Internet at <http://pubs.acs.org>.

OM0002834

(14) teXsan: Crystal Structure Analysis Package; Molecular Structure Corp., The Woodlands, TX, 1985 and 1992.

(15) PATY: Beurskens, P. T.; Admiraal, G.; Beurskens, G.; Bosman, W. P.; Garcia-Granda, S.; Gould, R. O.; Smits, J. M. M.; Smykalla, C. The DIRDIF Program System; Technical Report of the Crystallography Laboratory; University of Nijmegen, Nijmegen, The Netherlands, 1992.

(16) DIRDIF94: Beurskens, P. T.; Admiraal, G.; Beurskens, G.; Bosman, W. P.; de Gelder, R.; Israel, R.; Smits, J. M. M. The DIRDIF-94 Program System; Technical Report of the Crystallography Laboratory; University of Nijmegen, Nijmegen, The Netherlands, 1994.